JACS
JOURNAL OF THE AMERICAN CHEMICAL SOCIETY

ARTICLE

pubs.acs.org/JACS

Biomimetic Screening of Class-B G Protein-Coupled Receptors

Christian Devigny,[†] Francisco Perez-Balderas,[*,†,§] Bastiaan Hoogeland,[†] Serena Cuboni,[†] Rudolf Wachtel,[†] Christoph P. Mauch,[†] Katharine J. Webb,[†,‡] Jan M. Deussing,[†,‡] and Felix Hausch[*,†]

[†]Max-Planck-Institute of Psychiatry, Kraepelinstrasse 2-10, 80804 Munich, Germany

[‡]Institute of Developmental Genetics, Helmholtz Zentrum München, Ingolstaeter Landstrasse1, 85764 Neuherberg, Germany

Supporting Information

ABSTRACT: The 41-amino acid peptide corticotropin releasing factor (CRF) is a major modulator of the mammalian stress response. Upon stressful stimuli, it binds to the corticotropin releasing factor receptor 1 (CRF_1R), a typical member of the class-B G-protein-coupled receptors (GPCRs) and a prime target in the treatment of mood disorders. To chemically probe the molecular interaction of CRF with the transmembrane domain of its cognate receptor, we developed a high-throughput conjugation approach that mimics the natural activation mechanism of class-B GPCRs. An acetylene-tagged peptide library was synthesized and conjugated to an azide-modified high-affinity carrier peptide derived from the CRF C-terminus using copper-catalyzed dipolar cycloaddition. The resulting conjugates reconstituted potent agonists and were tested in situ for activation of the CRF_1 receptor in a cell-based assay. By use of this approach we (i) defined the minimal sequence motif that is required for full receptor activation, (ii) identified the critical functional groups and structure−activity relationships, (iii) developed an optimized, highly modified peptide probe with high potency (EC_{50} = 4 nM) that is specific for the activation domain of the receptor, and (iv) probed the behavioral role of CRF receptors in living mice. The membrane recruitment by a high-affinity carrier enhanced the potency of the tethered peptides by >4 orders of magnitude and thus allowed the testing of very weak initial fragments that otherwise would have been inactive on their own. As no chromatography purification of the test peptides was necessary, a substantial increase in screening throughput was achieved. Importantly, the peptide conjugates can be used to probe the endogenous receptor in its native environment in vivo.

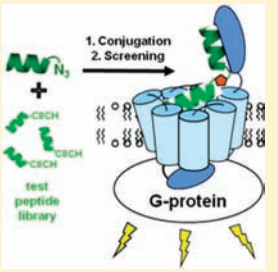

INTRODUCTION

Class-B G-protein-coupled receptors (GPCRs) of the secretin family (or subfamily B) comprise several important drug targets that are implicated in severe human diseases including diabetes, osteoporosis, neurodegeneration, inflammation, and psychiatric disorders.[1,2] Class-B GPCRs are without exception activated by large endogenous peptide hormones. Among them, corticotropin-releasing factor (CRF) is a 41-mer peptide that activates corticotropin-releasing factor receptor 1 (CRF_1R), a class-B GPCR that has been validated as a prime target in psychiatric disorders such as anxiety, depression, and addiction.[3−7] The general mechanism of ligand interaction with class-B GPCRs is based on a low resolution model termed the two-domain model (Figure 1a). All class-B GPCRs possess a large extracellular domain (ECD; ∼100−160 residues) with which they bind with high affinity to the carboxyl-terminal regions of their peptide ligands. This interaction serves as an anchorage for the peptide ligands.[2,8] A second interaction must occur between the juxtamembrane domain of the receptor and the amino-terminal portion of the peptide ligand that induces a structural rearrangement leading to intracellular G-protein activation.[9] In this model the intermediate part of the peptide ligands is thought to serve mainly as a connector between these two receptor binding sites.[10]

While the molecular binding mode between the ligand C-termini and the extracellular domains of class-B GPCRs is very well understood,[8] relatively little is known about the interaction between the peptide ligand N-termini and the juxtamembrane domains. The latter is a key issue not only to better understand the biochemistry of these receptors but also to advance drug discovery for this class of receptors. Herein we describe the use of peptide−peptide conjugates for a simple and rapid screening of the activation sequence motif for class-B GPCRs, using CRF_1R as a model system.

RESULTS AND DISCUSSION

We propose that the coupling of a CRF_1R extracellular domain specific C-terminal peptide with an N-terminal peptidic fragment could produce high potency agonists (Figure 1b). As C-terminal peptide we synthesized a cyclic 13 amino-acid peptide that possesses high affinity for the CRF_1R extracellular domain. This defined peptide is conjugated to variable probe fragments by copper-catalyzed chemical ligation. The coupling of the complementary azide and alkyne groups by "click-chemistry" should yield a peptide−peptide conjugate that effectively binds and activates the CRF receptor.

"Click" Peptide−Peptide Conjugates Ligands Are Full Activators of CRF_1R. Peptide **1** was designed as a high-affinity peptidic carrier based on an optimized C-terminal CRF analog and was synthesized by standard Fmoc SPPS (see Supporting Information).[11] This compound bears a fluorescent tag for quantification purposes and a triethylene glycol linker containing an azide group. Peptide **1** retains its high affinity (K_d = 18.8 ± 2.6 nM)

Received: January 7, 2011
Published: May 02, 2011

to the extracellular domain of CRF_1R (Figure S1 of Supporting Information). N-Terminal fragments, such as peptide **2**, were synthesized using a backbone amide linker (BAL) strategy in order to introduce an alkyne moiety at the peptide C-terminus.[12,13] The isolated peptide fragment **2** did not show any activity at the CRF_1R by itself up to a concentration of 10 μM in a cellular cAMP stimulation assay. The conjugation of peptide **2** with peptide **1** by copper catalyzed alkyne−azide cycloaddition, however, reconstituted a full agonist with a potency of 2.82 ± 0.23 nM (Figure 2). Thus the presented strategy constitutes a fast and efficient alternative to the synthesis of full length hormone derivatives. Moreover, the conjugation to the high-affinity carrier dramatically enhanced the detection limits for very weak agonists, such as fragment **2**, by at least 4 orders of magnitude.

Having proven that "clicked" conjugates can act as high potency agonists, we went on to determine the minimal peptide sequence that is necessary to fully activate the receptor. Bidirectionally truncated derivatives of peptide **2** were synthesized and coupled to peptide **1**. C-Terminal deletion of Arg^{15} led to a substantial decrease in potency. Surprisingly, N-terminal truncation of the conjugates initially increased potency. Truncation beyond Leu^5, however, completely abrogated the stimulating potency of the conjugates (Figure S2 and Table S1 of Supporting Information). These results established the 12-amino acid Ucn^{4-15} sequence motif (peptide **7**) as a good balance between size and potency. Conjugate **7** was thus used as a minimized activation segment and a starting point to further investigate the characteristics of CRF_1R activation.

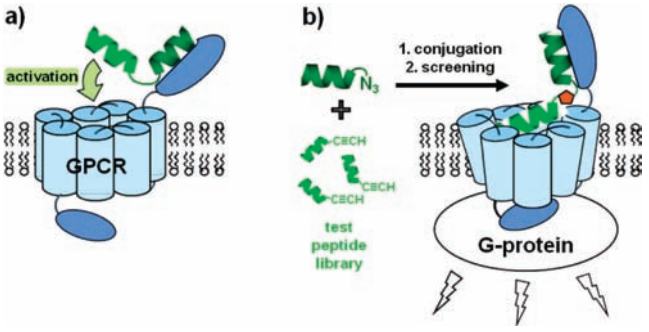

Figure 1. Mechanism of class-B GPCR signaling (a) and principle of biomimetic screening (b). (a) Mechanism of class-B GPCR signaling: The C-terminal part of the peptide ligand (dark green) binds with high affinity to the extracellular domain of the GPCR (dark blue). This recruits the N-terminal activation domain of the peptide ligand (light green) to the juxtamembrane domain of the GPCR leading to intracellular signal transduction.[9] (b) Biomimetic screening: A library of alkyne-tagged peptides (light green) is conjugated to a constant peptide fragment (dark green) that has high-affinity for the extracellular domain of the class-B GPCR. These conjugates are probed for modulation of the GPCR transmembrane domain.

Medium Throughput Screening of the Urocortin1 Activation Sequence. To explore the contribution of individual residues to CRF_1R stimulation in more detail we engaged on a medium throughput screening of peptide−peptide conjugates. On the basis of the minimized reference template **7** identified above, we synthesized a library of 96 peptidic fragments containing a series of single amino acid substitutions. Conveniently, the synthesis of this library was achieved using standard SPPS in a 96 deep-well plate allowing the fast and parallel synthesis of the 96 C-terminal propargylated activation fragments. Each position of the $Ucn1^{4-15}$ peptide sequence was systematically changed to alanine, aminoisobutyric acid (Aib), the corresponding D-amino acid, as well as five structurally related natural or unnatural amino acids (Table 1).

The crude $Ucn1^{4-15}$ analogs were coupled via their C-terminal alkyne group to the purified carrier peptide **1** via the previously described method. Gratifyingly, the peptide−peptide conjugates were routinely found to be much less soluble than their precursors allowing simple precipitation for their purification (Figure S3 of Supporting Information). HPLC analysis of the crude conjugates showed complete conversion of the carrier peptide **1** for all 96 conjugation reactions and acceptable purities (≥65%) for most crude conjugates (89 out of 96).[14] At this stage we decided to test these crude peptide−peptide conjugates directly in a cellular assay without any further purification. This was possible as any residual reaction components (e.g., Cu^+, *t*-butanol, or any remaining unconjugated peptide fragments) were minimal and were found not to disturb the cellular assay.

To ensure the suitability of this procedure we purified 14 conjugates, including sequences with enhanced activity as well as peptide conjugates with <65% purity, by HPLC and compared the activities of the purified conjugates in the cellular assay with their crude product counterparts. In all the cases, only minimal differences in activity were found between the crude and the purified peptide conjugates, thus validating the in situ screening approach (Figure S4 and Table S5 of Supporting Information).[14]

The biomimetic screening of the peptide conjugate library resulted in 70 conjugates where the stimulatory activity for CRF_1R was reduced or completely abolished (Table 1 and Table S4 of

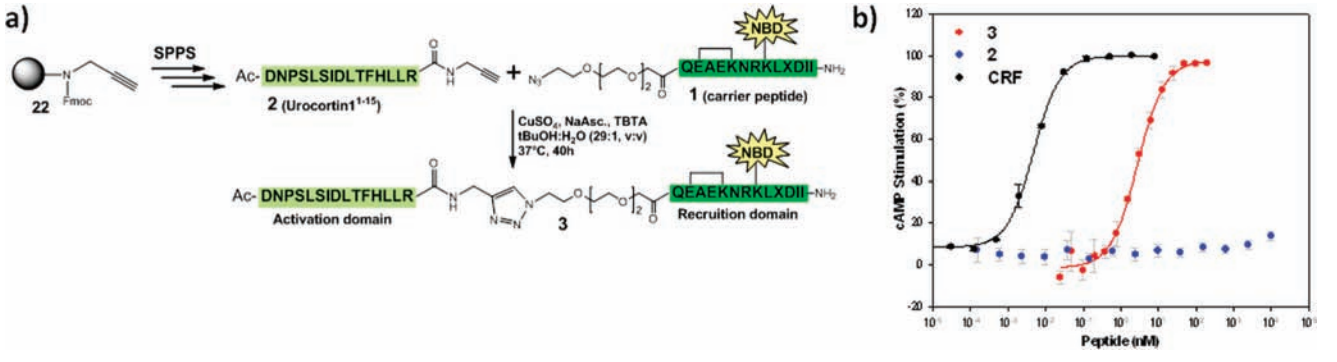

Figure 2. Stimulation of CRF_1R by a peptide−peptide conjugate. (a) Synthesis of the activation segment **2** (light green) using BAL resin **22** and "click" conjugation with membrane recruition segment **1** that is derived from CRF_1R ligands. X = cyclohexyl alanine, EAEK = lactam bridge, NBD = 4-(7-nitro)benzofurazanyl. (b) Stimulation of cAMP production in HEK293 cells stably overexpressing CRF_1R by peptide conjugate **3** and CRF.

dx.doi.org/10.1021/ja200160s |*J. Am. Chem. Soc.* 2011, 133, 8927–8933

Table 1. Summary of Single-Point Substitutions of the Ucn1$^{4-15}$ Sequence

Ser^4	Leu^5	Ser^6	Ile^7	Asp^8	Leu^9	Thr^{10}	Phe^{11}	His^{12}	Leu^{13}	Leu^{14}	Arg^{15}
Ala	Ala	Ala	Ala[(a)]	Ala	Ala	Ala	Ala	Ala	Ala	Ala	Ala
Aib	Aib	Aib	Aib	Aib	Aib	Aib	Aib	Aib	Aib	Aib	Aib
D-Ser	D-Leu	D-Ser	D-Ile	D-Asp[(a)]	D-Leu	D-Thr	D-Phe[(a)]	D-His	D-Leu	D-Leu	D-Arg
Thr[(a)]	Ile	Thr	Leu	Asn	Ile	Ser	Tyr[(a)]	Arg	Ile	Ile	Gln
Glu	Glu	Glu	Val[(a)]	Glu	Val	Glu	Trp	Glu	Val[(a)]	Val	Glu
Lys	Lys	Lys	Thr[(a)]	Thr	Phe	Lys	Lys	Lys	Phe	Phe	Lys
Dap	Cha[(a)]	Dap	Chg[(a)]	Dab	Cha	Dap	pI-Phe	Cha	Cha[(a)]	Cha	Cit
h-Ser	Nle	h-Ser	tBuGly	h-Ser	tBuAla[(a)]	h-Ser	PhGly[(a)]	h-Ser[(a)]	tBuAla	tBuAla	Orn

[a] These conjugates were additionally purified by high-performance liquid chromatography (HPLC) and retested for activity. Aib = α-aminoisobutyric acid; Cha = 3-cyclohexyl-L-alanine; Chg = L-α-cyclohexylglycine; Cit = L-citrulline; Dap = L-2,3-diaminopropionic acid; Dab = L-2,4-diaminobutyric acid; h-Ser = homoserine; Nle = norleucine; Orn = ornithine; PhGly = L-α-phenylglycine; pI-Phe = para-iodo phenylalanine; tBuAla = *β-tert*-butyl-L-alanine; tBuGly = L-α-*tert*-butylglycine. Crude peptide−peptide conjugates carrying the indicated amino acid change were assayed at 2 nM for cAMP stimulation of HEK293 cells stably overexpressing CRF$_1$R. Inactive sequences are indicated in red, minimal activity is indicated in orange, equal activity compared to the original Ucn1$^{4-15}$ conjugate **7a** is indicated in yellow, and activity-enhancing substitutions are highlighted in green.

Table 2. Binding to or Stimulation of CRF$_1$R (Cellular cAMP Production) by Multisubstituted Peptide Fragments and Conjugates (Mean ± Std Dev)

		R = carrier 1[a]			**R** = NH2[b]		
		EC$_{50}$ (nM) [c]		IC$_{50}$ (nM) [d]	EC$_{50}$ (nM) [c]		IC$_{50}$ (nM) [d]
		−15	**+15** (5 μM)	+I^{125}sauvagine (20pM)	**−15**	**+15** (5 μM)	+I^{125}sauvagine (20pM)
7	Ac-Ucn1$^{4-15}$-**R**	1.12 ± 0.05	Inact.[f]	5.4 ± 2.6	Inact.[g]	Inact.[h]	Inact.[e]
10	Ac-[Thr^{4}Cha^5]Ucn1$^{4-15}$-**R**	0.053 ± 0.001	7.1 ± 0.5	3.6 ± 1.8	487 ± 144[I]	Inact.[h]	Inact.[e]
11	Ac-[Thr^{4}Cha^{5}D-Phe^{11}]Ucn1$^{4-15}$-**R**	0.040 ± 0.001	5.1 ± 0.5	1.8 ± 0.9	181 ± 15	396 ± 31	10188 ± 6611
12	Ac-[Thr^{4}Cha^{5,13}D-Phe^{11}] Ucn1$^{4-15}$-**R**	0.074 ± 0.001	8.4 ± 0.5	2.2 ± 1.3	48 ± 2	113 ± 7	3738 ± 1604
13	Ac-[Thr^{4}Cha^{5,13}Chg^{7}D-Phe^{11}] Ucn1$^{4-15}$-**R**	0.037 ± 0.001	5.5 ± 0.3	1.6 ± 1.0	25 ± 1	50 ± 6	2977 ± 1602
14	Ac-[Thr^{4}Cha^{5,13}Chg^{7}tBuAla^{9}D-Phe^{11}] Ucn1$^{4-15}$-**R**	0.049 ± 0.001	5.9 ± 0.5	1.6 ± 0.6	4.0 ± 0.1	10.0 ± 1.0	400 ± 190

[a] Propargylated peptides conjugated to peptide **1**. [b] C-terminally amidated. [c] cAMP stimulation of a stable CRF$_1$R overexpressing cell line in the absence or presence of 5 μM of the extracellular domain-specific antagonist **15**. [d] Radioactive binding assay using membrane preparations from CRF$_1$R-overexpressing HEK293 cells. [e] Inactive up to 80 μM. [f] Inactive up to 50 nM . [g] Inactive up to 10 μM. [h] Inactive up to 5 μM. [I] Partial agonist.

Supporting Information). For 15 of these peptide conjugates, the CRF$_1$R stimulation was not significantly different compared to the wild-type sequence of Ucn1$^{4-15}$. However, an enhanced stimulation was observed for 11 peptide conjugates analogs. Analysis of the activities for the single amino acid substitution analogs allowed several conclusions about structure−activity relationship of CRF$_1$R agonist. First, the hydrogen bonding pattern of Arg^{15} seems to contribute to CRF$_1$R stimulation, consistent with the truncation study. Generally, positions 5, 7, 9, 13, and 14 tolerate only conservative aliphatic substitutions which can partially enhance potency. His^{12} seems to contribute comparatively less to the interaction with the CRF$_1$R receptor. An L- to D-Phe substitution at position 11 substantially improved the activity of the peptide conjugate. Interestingly, this substitution is also present in the high-affinity CRF$_1$R antagonist astressin.[15] The polar residues Ser^6, Asp^8, and to a lesser extent Thr^{10} are essential for activation, which is consistent with prior studies on full length CRF.[16,17] Ser^4 could be advantageously substituted for several amino acids.

Discovery of Agonists Specific for the Transmembrane Domain of CRF Receptors. The next step was to investigate whether the enhancing effects of the single substitutions identified above were additive. In the medium throughput screening, the substitutions Ser^{4}Thr, Leu^{5}Cha, and Phe^{11}D-Phe provided the greatest individual enhancement in potency. Combination of the first two mutations (**10a**) enhance potency 24-fold compared to the original urocortin$^{4-15}$ sequence (Table 2). The triple mutation in conjugate **11a** further slightly increased potency to provide a 40 pM agonist. Importantly, the combination of these point mutations showed for the first time detectable CRF$_1$R agonism in an untethered setup (peptides **10b** and **11b**, Table 2 and Figure S9 of Supporting Information). The successive incorporation of three additional mutations identified as beneficial in the single substitution screen (Ile^{7}Chg, Leu^{9}tBuAla, and

dx.doi.org/10.1021/ja200160s |*J. Am. Chem. Soc.* 2011, 133, 8927–8933

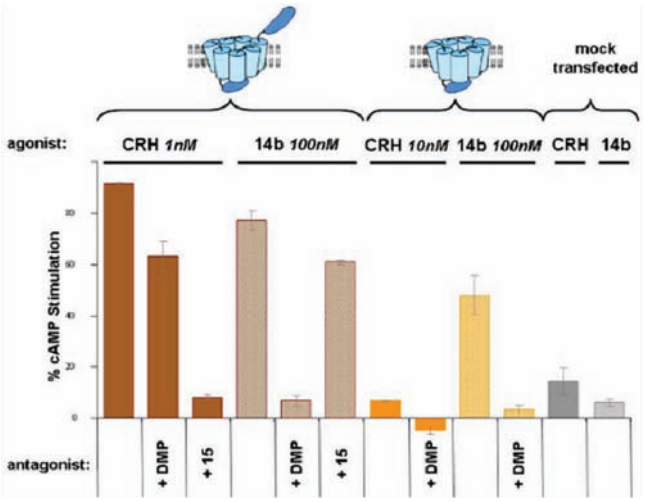

Figure 3. Stimulation of CRF_1R and extracellular domain-truncated CRF_1R by an optimized peptide agonist. HEK293 cells transiently overexpressing full length CRF_1R^{24-415} (brown bars), a truncated version $CRF_1R^{112-415}$ (yellow bars), or an empty vector (gray bars) were stimulated with CRF (filled) or peptide **14b** (hatched) at the indicated concentration in the absence or presence of the antagonists DMP696 (2 μM) or peptide **15** (Ac-EAEKNRKLXDII-NH_2,[11] X = Cha, underlined = lactam bridge, 10 μM). After 30 min, cAMP accumulation was determined and normalized to a negative (DMSO, 0%) and positive control (forskolin, 100%).

Leu[13]Cha) further enhanced the potency of untethered peptides to provide the hexasubstituted peptide **14b** as a low nanomolar agonist. From a structural point of view, it seems that this increase in potency was largely achieved by fine-tuning the hydrophobic interactions through incorporation of the unnatural amino acids side chains (Cha, Chg, and tBuAla). Intriguingly, these additional substitutions did not further increase the potency in the context of the high-affinity carrier. This is in contrast to the cooperative behavior classically expected for conjugated two-site binding fragments.[18] The molecular underpinnings for the apparent lower limit of approximately 50 pM for peptide-carrier **1** conjugates are currently unknown.

To confirm the specificity of peptide **14b** for CRF_1R in our test system, we first performed experiments using HEK293 cells transiently transfected with CRF_1R or mock controls. No significant cAMP stimulation could be detected in the latter setup (Figure 3). We further characterized the specificity of peptide **14b** by testing its ability to stimulate others class-B GPCRs. Peptide **14b** was active at the CRF_2R (34.1 $\pm$ 1.4 nM), the closest homologue of CRF_1R (>70% amino acid sequence identity). CRF_2R is also potently stimulated by the endogenous ligand Urocortin1 from which peptide **14b** was derived from, explaining the low degree of selectivity between the two CRF receptor subtypes. However, peptide **14b** was inactive in an assay using HEK293 cells transiently transfected with PTH_1R and GLP_1R, showing that there is no cross-reactivity for other closely related receptors (data not shown).

Pharmacological Characterization of Conjugates and Transmembrane-Specific Peptides. The N-terminal part of CRF corresponding to peptide **14b** is believed to primarily interact with the juxtamembrane domain of CRF_1R. To further characterize the binding mode of peptides **7b**−**14b** or of the corresponding conjugates we first performed cellular competition assays using peptide **15**,[11] which is an antagonist specific for the extracellular domain of CRF_1R (Table 2 and Figure 3). The cAMP stimulation potency of the conjugates was strongly reduced by a factor of 100 in the presence of 5.0 μM peptide **15**, a 200-fold excess compare to its K_i determined in the radioactive binding experiment (Figure S1 of Supporting Information). This is consistent with peptide **15** competitively inhibiting the binding of the carrier part of the conjugates to the extracellular domain, the latter being the dominating recognition event. For conjugate **7a**, the weakest of the conjugate series, no activity could be detected in the presence of inhibitor **15**. Likewise, CRF was strongly inhibited by peptide **15** (Figure 3). In contrast to the conjugates and CRF, the activities of the untethered peptides **10b**−**14b** were only mildly affected by a factor of 2.2 by the presence of 5.0 μM peptide **15** (Table 2 and Figure 3).

We next tested the conjugates and untethered peptides in HEK293 cells transiently overexpressing the full length CRF_1R or a truncated mutant lacking the extracellular domain (Table S2 of Supporting Information and Figure 3). While the results obtained using the full length construct nicely replicated those obtained using the stable CRF_1R overexpressing cell line for the conjugates and the untethered peptide series, substantial differences were found for the truncated mutant. In the latter system, none of the conjugates showed any remaining activity; neither did CRF (Table S2 of Supporting Information and Figure 3). The untethered peptides **10b**−**14b**, however, all activated the extracellular domain-deficient CRF_1R mutant, albeit with about 4-fold reduced potency. This clearly and directly shows that the transmembrane domain is the primary interaction site for these N-terminally derived CRF analogs, with only minor contributions from the extracellular domain, possibly indirectly by stabilizing the correct conformation of the juxtamembrane domain. It is noteworthy that the untethered peptides were able to stimulate the truncated CRF_1R mutant with good potency (e.g., 15.6 $\pm$ 0.5 nM for peptide **14b**), while their conjugated counterparts (e.g., **14a**) were inactive in the same setting. This could indicate that the carrier peptide **1** could actually negatively affect their conjugation partners when not bound to the extracellular domain.

To further characterize the interaction of peptide **14b** or conjugate **7a** with the transmembrane domain, we studied their sensitivity toward DMP696,[19] a nonpeptidic antagonist specific for the juxtamembrane domain (Figure 3, Figure 4, and Table S3 of Supporting Information). Increasing concentrations of DMP696 incrementally depressed the maximal stimulation (E_{max}) induced by **7a** while only weakly affecting the potency (EC_{50}) of the latter (Figure 4a), consistent with a noncompetitive mode of inhibition. This is in line with the two domain model were the receptor occupancy is largely determined by the extracellular domain and its high affinity to the carrier peptide (unaffected by DMP696), while efficacy is primarily determined by the interaction of the transmembrane domain and the conjugated N-terminal peptide. Importantly, the two-domain model predicts that concentrations of conjugate **7a** that fully saturate the extracellular domain constitute an upper limit to the effective ("intramolecular") concentration of the conjugated peptide **7** that can be "perceived" by the transmembrane domain. Further increasing concentrations of free conjugated **7a** unligated to the extracellular domain can be neglected in this context (Table 2 and Table S3 of Supporting Information, dECD). This maximal effective concentration of **7** is eventually unable to overcome the increasing concentrations of DMP696 (IC_{50} = 67 $\pm$ 5 nM for

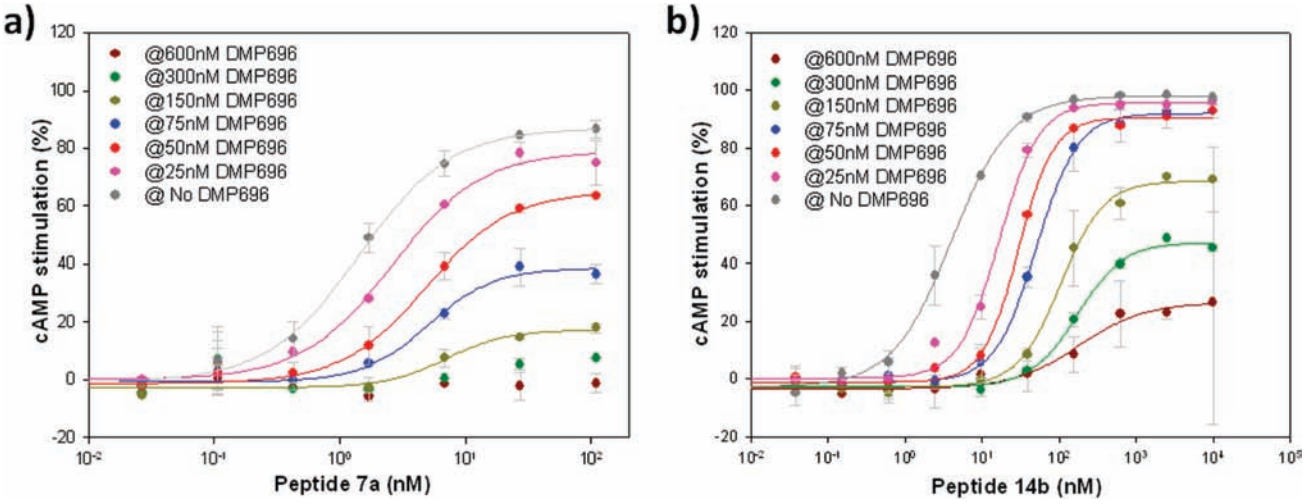

Figure 4. Mechanistic analysis of DMP696 inhibition vs peptide agonists **7a** and **14b**. Full dose−response curves for (a) conjugate **7a** and (b) peptide **14b** stimulated cAMP production in absence or presence of increasing concentrations of DMP696 using HEK293 cells stably overexpressing CRF_1R.

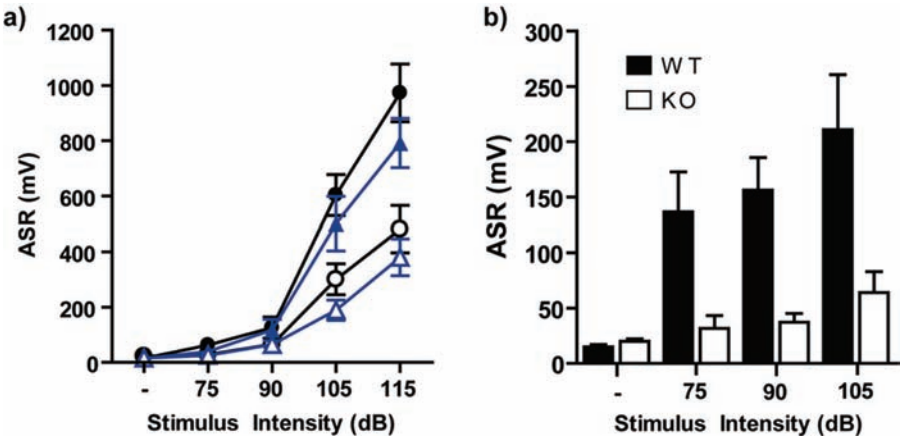

Figure 5. Acoustic startle response (ASR) in mice following intracerebroventricular injection of a peptide−peptide conjugate. Conjugate **7a** (0.16 μg, filled blue triangles), CRF (0.16 μg, filled black circles), and their corresponding vehicle controls (open triangles and circles, respectively) were injected directly into the lateral ventricle of mice, and the ASR was measured using increasing stimulus intensity (noise bursts). (a) CRF and conjugate **7a** injection led to significantly higher ASR than vehicle controls (105 and 115 dB, $p < 0.05$, respectively), but ASR increase by CRF did not differ significantly from that caused by conjugate **7a** ($p > 0.05$; statistical analyses were performed by 2-way repeated measures ANOVA, followed by Newman-Keuls posthoc test). (b) In comparison to wild-type mice conjugate **7a** was unable to increase the ASR in CRF_1R knockout mice. All data are shown as mean ± SEM.

depression of E_{max} of peptide **7a**) thus providing a mechanistic rationale for the observed noncompetitive mode of inhibition.

The sensitivity toward DMP696 was also investigated for the untethered multisubstituted agonist **14b** (Figures 3 and 4b) revealing an interaction reminiscent of a mixed competitive mode of inhibition. DMP696 strongly affected the EC_{50} of peptide **14b** even at low concentrations, while at higher concentrations it also reduced the E_{max} of the latter.

Finally, to probe the interaction the conjugates and untethered peptides to CRF_1R more directly competitive binding assays were performed with the natural peptide ligand I^{125}sauvagine (Table 2). All conjugates fully competed with the labeled tracer in the low nanomolar range, with only a modest increase in affinity with increasing degree of substitution in the conjugated N-terminal segment (compare IC_{50} = 5.4 ± 2.6 nM for **7a** to 1.6 ± 0.6 nM for **14a**). This is consistent with the constant carrier peptide **1** being the major driving force for binding and competition. The untethered peptides competed with I^{125}sauvagine only weakly, likely due to the lack of the high-affinity extracellular interaction and, only partially, reflecting a competition only with the fraction of I^{125}sauvagine that is bound to the high-affinity, γS-GTP-sensitive CRF_1R binding sites. The binding affinities of peptides **11b**−**14b**, however, were substantially improved with increasing degree of substitution, in line with the trend observed in the cAMP stimulation experiment. In all cases the affinities measured in the radioactive binding assays were substantially weaker than the potencies observed in the cAMP stimulation assays. This has been repeatedly observed also for the natural ligands CRF, urocortin, or sauvagine and possibly reflects a substantial receptor reserve in our CRF_1R overexpressing cells where only a small fraction of stimulated receptor is sufficient to fully activate the cellular secondary messenger machinery.

Biomimetic Targeting of Endogenous CRF_1R in Living Mice. A hallmark of the biomimetic screening approach presented here

dx.doi.org/10.1021/ja200160s |*J. Am. Chem. Soc.* 2011, 133, 8927–8933

is the possibility to target the unmodified native receptors. The peptide−carrier conjugates should therefore also be applicable to the endogenous receptors in their native environment. To test the effects of conjugates in a physiologically relevant system, the conjugate **7a** (Ucn1$^{4-15}$) was administered directly to the brain of wild-type mice via intracerebroventricular injection. The CRF_1R-mediated modulation of the stress response was then evaluated using the acoustic startle response (ASR) paradigm (Figure 5a).[20] Gratifyingly, the sensitizing effects of the peptide conjugate on the startle response were qualitatively similar to exogenously applied CRF controls. Moreover, CRF_1R knockout mice did not respond to the injection of peptide conjugate **7a** (Figure 5b), thus proving the specificity of the synthetic peptide conjugates for the endogenous CRF_1 receptor in vivo. Likewise, the potentiation in startle response was also observed after injection of the optimized, juxtamembrane-specific agonist **14b**, again in a CRF1R-dependent manner (Figure S5 of Supporting Information).

CONCLUSIONS

In this work we developed a rapid approach to chemically probe the activation domain of class-B GPCRs. We show that the conjugation of a high affinity carrier results in a dramatic enhancement in activity. This allows the initial testing of peptides whose activity would otherwise have been too weak to be detectable. The synthesis and coupling of short length peptides to reconstitute a fully functional CRF_1R modulator has several advantages compared to the classical synthesis of whole, full length peptide ligands. For example, it is quicker with higher product purities. Importantly, the fragment conjugation approach obviated the need for HPLC purification of the initial test peptides, thereby enabling a substantially higher screening throughput. The crude peptide conjugates were compatible with functional assays in living cells. This was likely facilitated in part by the exquisite target receptor specificity of the conjugates imparted by the carrier. This also enabled the straightforward extension of this concept to very complex biological systems, such as whole animal models.

By application of this methodology to the class-B GPCR CRF_1R we discovered a low nanomolar agonist that is specific for the activation domain of this receptor. The activation mechanism of peptide **14b** is almost independent of the extracellular domain and resembles the signaling mechanism of canonical class A GPCRs. We assume that peptide **14b** binds at the endogenous hormone orthosteric site and derives its activity from optimized hydrophobic interactions. Our results are inconsistent with a necessary allosteric change of the extracellular domain which had been postulated as the initiating step of signal transduction for other class-B GPCRs.[21,22] CRF_1R therefore resembles more closely the parathyroid hormone receptor 1—the only other class-B GPCR for which juxtamembrane-specific ligands have been described.[23,24] Whether transmembrane-specific agonists for other class-B GPCRs can be identified by the method described in this manuscript remains to be determined.

Given the high mechanistic and structural homology within the class-B GPCR family,[2,8] we expect the biomimetic screening approach to be applicable to many class-B GPCRs. The key principle of this study—testing class-B ligands after membrane recruitment—is related in some aspects to a recently published "mammalian class-B ligand display".[25] However, while potentially superior in the number of tested peptides, the latter approach is inherently limited to genetically encoded amino acids. It is noteworthy that—at least in this example for CRF_1R—five unnatural amino acids substitutions were necessary to achieve low nanomolar, juxtamembrane-specific ligands. As such the "carrier-conjugate" approach presented in this study might be better suited to produce hits for drug development, as this method can be readily adapted to unnatural or even nonpeptidic test substances.

EXPERIMENTAL METHODS

Standard Procedure for the Conjugation of Peptides. The peptidic carrier **1** (1 mM solution in acetonitrile/water 50/50, v/v) (15 nmol) and the desired propargylated N-terminal peptide (1 mM solution in acetonitrile/water 50/50, v/v) (4 equiv, 60 nmol) were transferred to a reaction tube (1.5 mL). The mixture was evaporated under reduced pressure. The residue was dissolved in tert-butanol/water (43/1, v/v, 722 μL); sonication was used to help peptide dissolution where necessary. To this solution were added sequentially TBTA (1 mM solution in tert-butanol/water 43/1, v/v, 1.3 equiv., 20 nmol, 20 μL), sodium ascorbate (71 mM solution in water, 28 equiv, 412 nmol, 5.8 μL), and copper sulfate (140 mM solution in water, 21 equiv, 308 nmol, 2.2 μL). The mixture was shaken for 40 h at 37 °C. The tube was cooled down to room temperature and then centrifugated (13000 rpm, 5 min). The supernatant was removed by decantation and the precipitate was washed with tert-butanol/water (43/1, v/v, 100 μL). The precipitate was dried under vacuum. The crude conjugates were dissolved in DMSO and analyzed by reverse-phase HPLC.

cAMP Stimulation Assay. For the stimulation assay, cells grown to 50−60% confluency in DMEM (+ FCS 10%, penicillin/streptomycin) were detached from the culture dish with Cell dissociation solution (Sigma, Germany), resuspended in stimulation buffer (SB, 5 mM HEPES, 0,1% BSA, 0.1 mM IBMX in HBSS), and seeded in 5 μL into a Corning 384 well plate (#3572) at a density of 3000 cells/well. After equilibration for 10 min at room temperature, 5 μL of SB containing peptides and/or DMSO, forskolin, or DMP696 (generous gift by Bristol-Myers-Squibb) were added. After incubation for 30 min at room temperature, cells were lysed, and the cAMP content was measured using the cAMP dynamic HTRF detection kit (CisBio, France) according to the manufactures instructions and using a Tecan Genios Pro equipped with 320/35 nm excitation and 620/10 nm and 665/8 nm emission filters. The ratiometric fluorescence signals obtained were normalized to the positive (forskolin, 100%) and negative controls (DMSO, 0%). Additional information on cell culture, transfection conditions, and constructs used are available in the Supporting Information.

ASR. ASR testing was carried out as described in Golub et al.[20] Briefly, mice injected with either peptide or vehicle were subjected to noise impulses of increasing intensities (75, 90, 105, and 115 dB(A)) in a SR-LAB (San Diego Instruments) apparatus with background noise set to 50 dB(A). The data depicted on the graphs represent the mean peak startle amplitude in mV ± SEM in response to 30 pulses of each intensity as well as 12 background (BG) noise measurements. The effect of the conjugate **7a** on the ASR in comparison to CRF was studied in Crhr1$^{flox/flox}$ control mice obtained from breedings of conditional CRF1R knockout mice as previously described (n = 9−12).[26] The data were subsequently subjected to 2-way repeated measures ANOVA followed by Newman-Keuls posthoc test. Moreover, to assess the specificity of peptides **7a** and **14b**, the ASR response of constitutive CRF_1R knockout mice (n = 2−3)[27] was measured in comparison to wild-type littermates (n = 3−4). The guide cannulas for the intracerebroventricular injections were implanted in anaesthetised mice secured in a stereotaxic frame. The skull surface was exposed, and a 23 gauge guide cannula, 8 mm in length, was inserted using the following coordinates: 0.3 mm posterior from

bregma (AP), 1 mm lateral distance from the midline (L), and 1.2 mm deep from the level of the skull surface (DV). The animals were left to recover for at least ten days before testing.

Data Analysis. SigmaPlot software version 11.0 was used for sigmoidal curve fitting of ligand concentration−response curves and for calculating the EC_{50} values as an index of ligand potency. The statistical parameters were generated from a composite nonlinear regression (four parameter logistic curve, SigmaPlot) of pooled data from two independent samples. In general, the mean and the standard deviation were expressed for values obtained from duplicate samples. The cAMP production response was normalized to a positive control (Forskolin, 100%) and a negative control (DMSO, 0%). GraphPad Prism software version 5.0 was used for curve fitting of the acoustic startle response in mice and statistical analysis of variance.

■ ASSOCIATED CONTENT

Supporting Information. Information about experimental procedures, full references, analytical and spectral characterization data, cAMP stimulation assays, and animal experiments. This material is available free of charge via the Internet at http://pubs.acs.org.

■ AUTHOR INFORMATION

Corresponding Author

hausch@mpipsykl.mpg.de; francisco.perez-balderas@rob.ox.ac.uk

Present Addresses

[§]CR/UK Gray Institute for Radiation Oncology and Biology, Department of Oncology, University of Oxford, Old Road Campus Research Building, Off Roosevelt Drive, Churchill Hospital, Oxford OX3 7DQ, United Kingdom

■ ACKNOWLEDGMENT

We thank Mrs. E. Weyher and Dr. S. Uebel (MPI of Biochemistry, Martinsried, Germany), Dr. G. Maccarone and Pr. Dr. C. Turck (MPI of Psychiatry, Munich, Germany) for MS analysis, and Mrs. C. Dubler (Ludwig-Maximilians-Universität München) for NMR measurements. We are indebted to Prof. F. Holsboer for generous support. This work was partially supported by the Chemical Genomics Centre (Dortmund), by the Bundesministerium für Bildung und Forschung within the framework of the NGFN-Plus (FKZ: 01GS08155), and by the Initiative and Networking Fund of the Helmholtz Association in the framework of the Helmholtz Alliance for Mental Health in an Ageing Society (HA-215).

■ REFERENCES

(1) Foord, S. M.; Jupe, S.; Holbrook *J. Biochem. Soc. Trans.* **2002**, *30*, 473.
(2) Hoare, S. R. *Drug Discov. Today* **2005**, *10*, 417.
(3) Holsboer, F. *Neuropsychopharmacology* **2000**, *23*, 477.
(4) Bale, T. L.; Vale, W. W. *Annu. Rev. Pharmacol. Toxicol.* **2004**, *44*, 525.
(5) Grigoriadis, D. E. *Expert Opin. Ther. Targets* **2005**, *9*, 651.
(6) Holsboer, F.; Ising, M. *Annu. Rev. Psychol.* **2010**, *61*, 81.
(7) Koob, G. F.; Zorrilla, E. P. *Curr. Opin. Invest. Drugs* **2010**, *11*, 63.
(8) Parthier, C.; Reedtz-Runge, S.; Rudolph, R.; Stubbs, M. T. *Trends Biochem. Sci.* **2009**, *34*, 303.
(9) The juxtamembrane domain is defined as the extracellular loops and the extracellular facing parts of the transmembrane helices of GPCRs.
(10) Beyermann, M.; Rothemund, S.; Heinrich, N.; Fechner, K.; Furkert, J.; Dathe, M.; Winter, R.; Krause, E.; Bienert, M. *J. Biol. Chem.* **2000**, *275*, 5702.
(11) Yamada, Y.; Mizutani, K.; Mizusawa, Y.; Hantani, Y.; Tanaka, M.; Tanaka, Y.; Tomimoto, M.; Sugawara, M.; Imai, N.; Yamada, H.; Okajima, N.; Haruta, J. *J. Med. Chem.* **2004**, *47*, 1075.
(12) Jensen, J. A.; Songster, M. F.; Vágner, J.; Albericio, F.; Barany, G. *J. Am. Chem. Soc.* **1998**, *120*, 5441.
(13) Springer, J.; Kimberly, R. d. C.; Sandrine, C. V.; Jan, A. J. G.; Pedro, H. H. H.; Henk, H.; Jan, H. v. M. *Eur. J. Org. Chem.* **2008**, No. 15, 2592.
(14) The Ucn^{4-15} sequence had a pronounced tendency to form an isomer with higher polarity which was the major impurity for most Ucn analogs. Purified samples of selected isomeric conjugates were found to stimulate CRF_1R with equal potency compared to their corresponding correct isomers.
(15) Gulyas, J.; Rivier, C.; Perrin, M.; Koerbe, S. C.; Sutton, S.; Corrigan, A.; Lahrichi, S. L.; Craig, A. G.; Vale, W. W.; Rivier, J. E. *Proc. Natl. Acad. Sci. U.S.A.* **1995**, *92*, 10575.
(16) Kornreich, W. D.; Galyean, R.; Hernandez, J. F.; Craig, A. G.; Donaldson, C. J.; Yamamoto, G.; Rivier, C.; Vale, W. W.; Rivier, J. E. *J. Med. Chem.* **1992**, *35*, 1870.
(17) Beyermann, M.; Fechner, K.; Furkert, J.; Krause, E.; Bienert, M. *J. Med. Chem.* **1996**, *39*, 3324.
(18) Murray, C. W.; Verdonk, M. L. *J. Comput. Aided Mol. Des.* **2002**, *16*, 751.
(19) He, L.; Gilligan, P. J.; Zaczek, R.; Fitzgerald, L. W.; McElroy, J.; Shen, H. S.; Saye, J. A.; Kalin, N. H.; Shelton, S.; Christ, D.; Trainor, G.; Hartig, P. *J. Med. Chem.* **2000**, *43*, 449.
(20) Golub, Y.; Mauch, C. P.; Dahlhoff, M.; Wotjak, C. T. *Behav. Brain Res.* **2009**, *205*, 544.
(21) Dong, M.; Pinon, D. I.; Asmann, Y. W.; Miller, L. J. *Mol. Pharmacol.* **2006**, *70*, 206.
(22) Dong., M.; Gao, F. D.; Pinon, D. I.; Miller, L. J. *Mol. Endocrinol.* **2008**, *22*, 1489.
(23) Shimizu, M.; Potts, J. T., Jr.; Gardella, T. J. *J. Biol. Chem.* **2000**, *275*, 21836.
(24) Carter, P. H.; et al. *Proc. Natl. Acad. Sci. U.S.A.* **2007**, *104*, 6846.
(25) Fortin, J.-P.; Zhu, Y.; Choi, C.; Beinborn, M.; Nitabach, M. N.; Kopin, A. S. *Proc. Natl. Acad. Sci. U.S.A.* **2009**, *106*, 8049.
(26) Müller, M. B.; et al. *Nat. Neurosci.* **2003**, *6*, 1100.
(27) Timpl, P.; Spanagel, R.; Sillaber, I.; Kresse, A.; Reul, J. H. M.; Stalla, G. K.; Blanquet, V.; Steckler, T.; Holsboer, F.; Wurst, W. *Nat. Genet.* **1998**, *19*, 162.